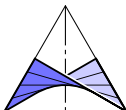


Multistable Design of Triangulated Cones

Georg Nawratil^{1,2}

¹Institute of Discrete Mathematics and Geometry, TU Wien
www.dmg.tuwien.ac.at/nawratil/

²Center for Geometry and Computational Design, TU Wien



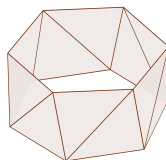
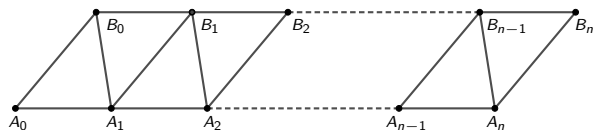
Introduction

Circular arrangement of the Kresling pattern

The strip has finite length and is folded such that $A_0 = A_n$ and $B_0 = B_n$ holds ($n \geq 3$) and that A_1, \dots, A_n and B_1, \dots, B_n form regular n -gons.

This discretized cylindrical strip has a bi-stable behavior according to Wunderlich [13], where these structures appear as special cases (regular ones) of snapping anti-prisms.

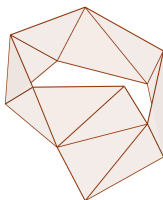
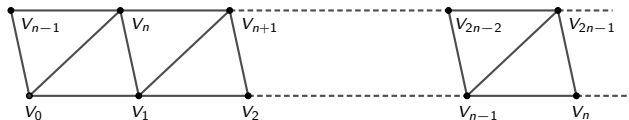
These snapping regular anti-prisms can be composed repetitively to cylindrical towers [1, 3, 5, 6].



Helical arrangement of the Kresling pattern

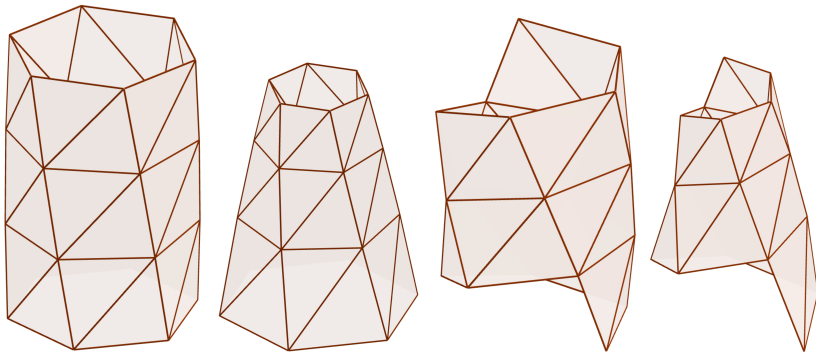
The strip can be assumed of infinite length where every label V_i with $i \geq n - 1$ ($n \geq 3$) appears twice (once on the lower rim and once on the upper one). One can fold up the strip in a way that points with the same labels match and are located on a helix.

The resulting triangulated cylinder studied in [2, 12] are multi-stable and from the formulation used in [12], it can be seen that there exists in general $n - 2$ cylindrical realizations (without taking reality or self-intersections into account).



Rough goal

Generalize these two constructions for conical structures, i.e. vertices are located on a cone of revolution, which can e.g. be used as reconfigurable antenna [7] or foldable horn speakers [11].



Review on the triangulated conical structures

They are studied in a journal article of Ishida et al. [4] and a presentation manuscript of Nojima [9] (which are based on three works written in Japanese).

In [4] the crease patterns of conical structures are generated from crease patterns of cylindrical structures by applying planar conformal maps. This approach does not allow direct access to its spatial conical shape, with exception of the flat foldable state, which can be added as an extra condition to the crease pattern (cf. [Eq. (14),4]).

Review on the triangulated conical structures

They are studied in a journal article of Ishida et al. [4] and a presentation manuscript of Nojima [9] (which are based on three works written in Japanese).

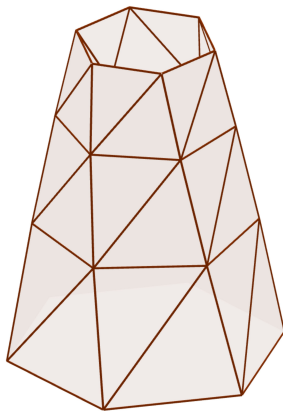
In [4] the crease patterns of conical structures are generated from crease patterns of cylindrical structures by applying planar conformal maps. This approach does not allow direct access to its spatial conical shape, with exception of the flat foldable state, which can be added as an extra condition to the crease pattern (cf. [Eq. (14),4]).

We do not generate the planar crease pattern but construct directly the triangulation on the 3-dimensional shape (cone).

Kinematic construction

We sliced the cone along parallel planes orthogonal to the rotation axis and discretize the resulting circles by regular n -gons, where adjacent ones are connected in the combinatorics of an antiprism. We call these objects **regular anti-frusta**.

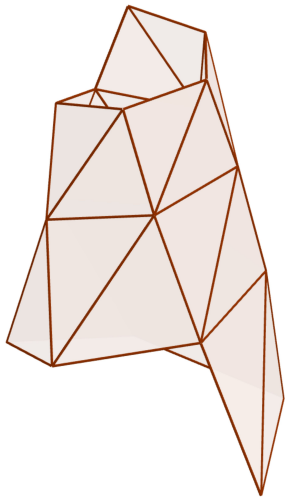
To archive periodicity of the structure we demand that each anti-frustum can be transformed into any other one by a so-called **spiral displacement** σ ; i.e. composition of a rotation about the cone axis and a scaling with center in the apex.



Kinematic construction

We start with a line-segment V_0V_1 with non-zero slope, whose end points are located on the cone. Now we apply a **spiral displacement** σ to this line segment, in such a way that $\sigma(V_0) = V_1$ holds.

By iterating the process, i.e. $\sigma^i(V_0) = \sigma^{i-1}(V_1)$, we get all vertices of the structure, which are located on a so-called concho-spiral (or conical helix). In the remainder of the talk we will name this curve a spiral for short.

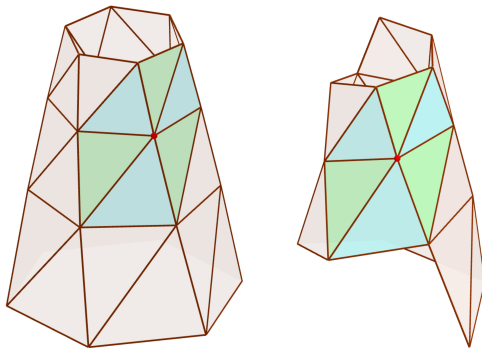


Triangulated cones are origami structures

A cone is a developable surface, but also the proposed triangulations of the cone are developable:

The triangulated cone consists of two types of triangles with respect to spiral displacements.

In every vertex all six angles determined by these two triangles meet and sum up to 2π .



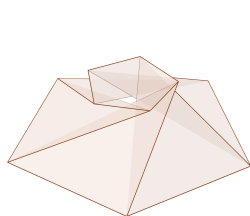
Shaky and snapping realizations

In general, there exists a finite number of realizations of such a conical framework; i.e. they are multistable.

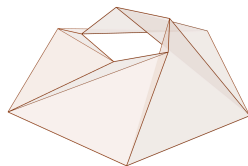
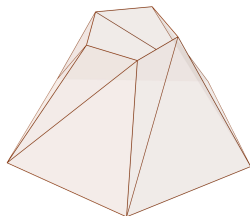
Shaky and snapping realizations

In general, there exists a finite number of realizations of such a conical framework; i.e. they are multistable.

A realization is called a **snapping realization** if it is close enough to another incongruent realization such that the physical model can snap into this neighboring realization due to non-destructive elastic deformations of material. It is well-known that **infinitesimal flexibility** can be seen as the limiting case where two realizations coincide.

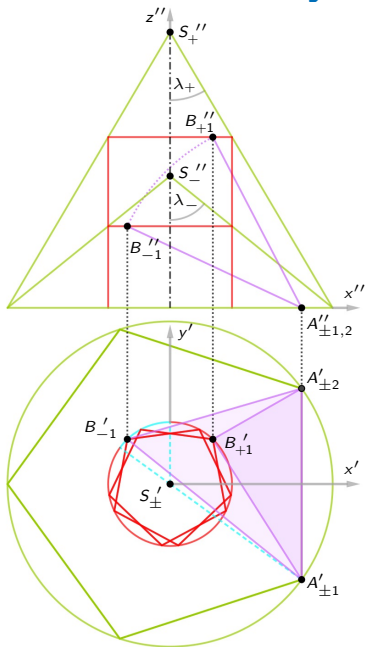


Snapping anti-frustum



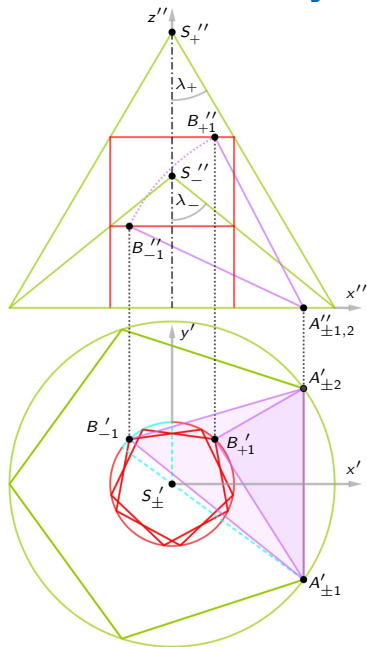
Shaky anti-frustum

Construction of shaky and snapping anti-frusta



Shaky and snapping regular anti-frusta correspond to special cases in the study of Wunderlich [13].

Construction of shaky and snapping anti-frusta



Shaky and snapping regular anti-frusta correspond to special cases in the study of Wunderlich [13].

Therefore we will focus on spiral-motion based conical triangulations in the remainder of the talk.

Outline

1. Algebraic formulation
2. Realizations on different cones
3. Two realizations on the same cone
 - a. Shaky realizations
 - b. On self-intersection free realizations
4. Orthogonal cross sections
5. Snappability computation
6. Open problems & References

1. Parametrization

We start with a parametrization of the spiral, which reads as:

$$\mathbf{s}(\varphi) = \begin{pmatrix} re^{m\varphi} \cos \varphi \\ re^{m\varphi} \sin \varphi \\ -re^{m\varphi} \cot \lambda \end{pmatrix} \quad \text{with } r > 0 \quad \text{and} \quad m = \sin \lambda \cot \delta$$

where $\delta \in]\frac{\pi}{2}, \pi[$ is the angle between the spiral tangent and the corresponding generator of the cone with half apex angle λ . We consider the part of the spiral which starts below the xy -plane (for $\varphi = 0$) and winds up (math. positive) to the origin for $\varphi \rightarrow \infty$.

1. Parametrization

We start with a parametrization of the spiral, which reads as:

$$\mathbf{s}(\varphi) = \begin{pmatrix} re^{m\varphi} \cos \varphi \\ re^{m\varphi} \sin \varphi \\ -re^{m\varphi} \cot \lambda \end{pmatrix} \quad \text{with } r > 0 \quad \text{and} \quad m = \sin \lambda \cot \delta$$

where $\delta \in]\frac{\pi}{2}, \pi[$ is the angle between the spiral tangent and the corresponding generator of the cone with half apex angle λ . We consider the part of the spiral which starts below the xy -plane (for $\varphi = 0$) and winds up (math. positive) to the origin for $\varphi \rightarrow \infty$.

Two different spatial states \mathcal{R}_+ and \mathcal{R}_- of our vertex set V_i :

$$V_{\pm i} = \begin{pmatrix} r_{\pm} p_{\pm}^i \cos(i\varphi_{\pm}) \\ r_{\pm} p_{\pm}^i \sin(i\varphi_{\pm}) \\ -r_{\pm} p_{\pm}^i q_{\pm} \end{pmatrix} \quad p_{\pm} := e^{\varphi_{\pm} \sin \lambda_{\pm} \cot \delta_{\pm}}, \quad q_{\pm} = \cot \lambda_{\pm}$$

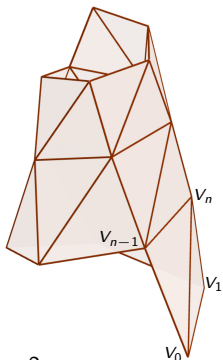
for fixed $\varphi_-, \varphi_+ \in]0; \pi[$ and $r_+ = 1$.

1. Set of equations

The lengths of corresponding edges have to agree, which yields an infinite set \mathcal{E} of equations $d(i, j) = 0$ with $d(i, j) := \overline{V_{+i}V_{+j}}^2 - \overline{V_{-i}V_{-j}}^2$.

As the complete edge set can be generated by the spiral displacement of the three edges $V_{\pm 0}V_{\pm 1}$, $V_{\pm 0}V_{\pm(n-1)}$ and $V_{\pm 0}V_{\pm n}$, the following relations hold for $k \in \mathbb{N}$:

$$\begin{aligned}d(k, k+1) &= p_+^{2k} \overline{V_{+0}V_{+1}}^2 - p_-^{2k} \overline{V_{-0}V_{-1}}^2 \\d(k, k+n-1) &= p_+^{2k} \overline{V_{+0}V_{+(n-1)}}^2 - p_-^{2k} \overline{V_{-0}V_{-(n-1)}}^2 \\d(k, k+n) &= p_+^{2k} \overline{V_{+0}V_{+n}}^2 - p_-^{2k} \overline{V_{-0}V_{-n}}^2\end{aligned}$$



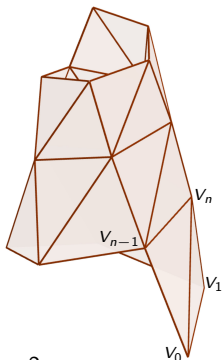
1. Set of equations

The lengths of corresponding edges have to agree, which yields an infinite set \mathcal{E} of equations $d(i, j) = 0$ with $d(i, j) := \overline{V_{+i}V_{+j}}^2 - \overline{V_{-i}V_{-j}}^2$.

As the complete edge set can be generated by the spiral displacement of the three edges $V_{\pm 0}V_{\pm 1}$, $V_{\pm 0}V_{\pm(n-1)}$ and $V_{\pm 0}V_{\pm n}$, the following relations hold for $k \in \mathbb{N}$:

$$\begin{aligned}d(k, k+1) &= p_+^{2k} \overline{V_{+0}V_{+1}}^2 - p_-^{2k} \overline{V_{-0}V_{-1}}^2 \\d(k, k+n-1) &= p_+^{2k} \overline{V_{+0}V_{+(n-1)}}^2 - p_-^{2k} \overline{V_{-0}V_{-(n-1)}}^2 \\d(k, k+n) &= p_+^{2k} \overline{V_{+0}V_{+n}}^2 - p_-^{2k} \overline{V_{-0}V_{-n}}^2\end{aligned}$$

This already implies, that \mathcal{E} can only have a solution for $p := p_- = p_+$ as $p_{\pm} \in]0; 1[$ has to hold (for reasons of reality).



1. The three basic equations

This boils down the problem to the solution of the equations $d(0, 1) = 0$, $d(0, n - 1) = 0$ and $d(0, n) = 0$. By using **Chebyshev polynomials of the first kind** $T_i(x)$, which are recursively defined by:

$$T_{i+1}(x) = 2xT_i(x) - T_{i-1}(x) \quad \text{with} \quad T_0(x) = 1 \quad \text{and} \quad T_1(x) = x,$$

we can rewrite $d(0, k)$ for $k = 1, n - 1, n$ under consideration of $T_i(\cos \varphi_{\pm}) = \cos(i\varphi_{\pm})$ by

$$d(0, k) = (p^{2k} q_+^2 - 2p^k q_+^2 - 2T_k(c_+)p^k + p^{2k} + q_+^2 + 1) - \\ (p^{2k} q_-^2 - 2p^k q_-^2 - 2T_k(c_-)p^k + p^{2k} + q_-^2 + 1)r_-^2$$

with $c_{\pm} = \cos \varphi_{\pm}$. By the conducted substitutions $d(0, k)$ turns into an algebraic expression in the variables p, q_{\pm}, c_{\pm}, r_- , where q_+ and q_- are known design inputs.

2. Two realizations on different cones

By eliminating r_- and p from the three basic equations, one ends up with a planar algebraic curve $h(c_-, c_+)$. We distinguish two cases:

1. **General case:** None of the two cones degenerate to a plane. The planar curve h is of degree $n^2 - 9$.
2. **Special case:** One of the two cones degenerates to a plane. The planar curve h is of degree $(n - 1)^2 - 4$.

2. Two realizations on different cones

By eliminating r_- and p from the three basic equations, one ends up with a planar algebraic curve $h(c_-, c_+)$. We distinguish two cases:

- 1. General case:** None of the two cones degenerate to a plane. The planar curve h is of degree $n^2 - 9$.
- 2. Special case:** One of the two cones degenerates to a plane. The planar curve h is of degree $(n - 1)^2 - 4$.

Remark 1: Multi-stable designs can only exist for $n > 3$.

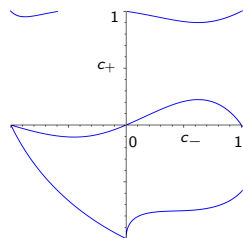
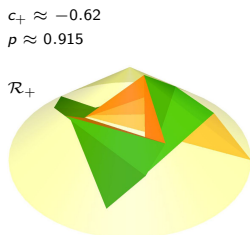
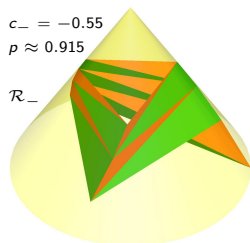
2. Two realizations on different cones

By eliminating r_- and p from the three basic equations, one ends up with a planar algebraic curve $h(c_-, c_+)$. We distinguish two cases:

- 1. General case:** None of the two cones degenerate to a plane. The planar curve h is of degree $n^2 - 9$.
- 2. Special case:** One of the two cones degenerates to a plane. The planar curve h is of degree $(n - 1)^2 - 4$.

Remark 1: Multi-stable designs can only exist for $n > 3$.

Example 1: $n = 4$, $\lambda_- = \frac{\pi}{6}$ and $\lambda_+ = \frac{\pi}{3} \implies h$ is a septic



3. Three realizations on different cones

The existence of a one-parametric solution curve h for the design of bi-stable conical structures allows theoretically the design of tri-stable ones. We index the third realization by the symbol \circ .

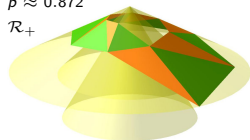
3. Three realizations on different cones

The existence of a one-parametric solution curve h for the design of bi-stable conical structures allows theoretically the design of tri-stable ones. We index the third realization by the symbol \circ .

Example 2: $n = 7$ and $\lambda_+ = \frac{\pi}{3}$, $\lambda_\circ = \frac{\pi}{4}$, $\lambda_- = \frac{\pi}{6}$.

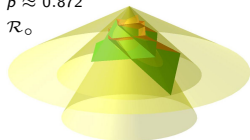
$$c_+ \approx 0.642$$

$$p \approx 0.872$$

$$\mathcal{R}_+$$


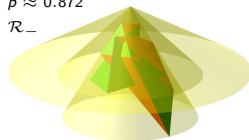
$$c_\circ \approx -0.016$$

$$p \approx 0.872$$

$$\mathcal{R}_\circ$$


$$c_- \approx -0.141$$

$$p \approx 0.872$$

$$\mathcal{R}_-$$


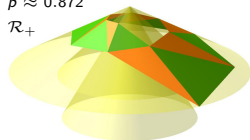
3. Three realizations on different cones

The existence of a one-parametric solution curve h for the design of bi-stable conical structures allows theoretically the design of tri-stable ones. We index the third realization by the symbol \circ .

Example 2: $n = 7$ and $\lambda_+ = \frac{\pi}{3}$, $\lambda_\circ = \frac{\pi}{4}$, $\lambda_- = \frac{\pi}{6}$.

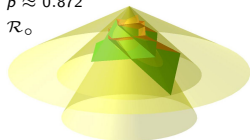
$$c_+ \approx 0.642$$

$$p \approx 0.872$$

$$\mathcal{R}_+$$


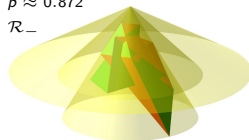
$$c_\circ \approx -0.016$$

$$p \approx 0.872$$

$$\mathcal{R}_\circ$$


$$c_- \approx -0.141$$

$$p \approx 0.872$$

$$\mathcal{R}_-$$


Remark 2: We were not able to find examples where all three realizations are free of self-intersections.

3. Two realizations on the same cone

We set $q := q_+ = q_-$ and do the same elimination as before ending up with the algebraic curve $h(c_-, c_+)$. We distinguish two cases:

1. **General case:** $q \neq 0$.

The planar curve h is of degree $n(n-1) - 6$.

2. **Special case:** $q = 0$

The planar curve h is of degree $(n-2)(n-3)$.

3. Two realizations on the same cone

We set $q := q_+ = q_-$ and do the same elimination as before ending up with the algebraic curve $h(c_-, c_+)$. We distinguish two cases:

1. **General case:** $q \neq 0$.

The planar curve h is of degree $n(n-1) - 6$.

2. **Special case:** $q = 0$

The planar curve h is of degree $(n-2)(n-3)$.

Remark 3: Multi-stable designs can only exist for $n > 3$.

3. Two realizations on the same cone

We set $q := q_+ = q_-$ and do the same elimination as before ending up with the algebraic curve $h(c_-, c_+)$. We distinguish two cases:

1. **General case:** $q \neq 0$.

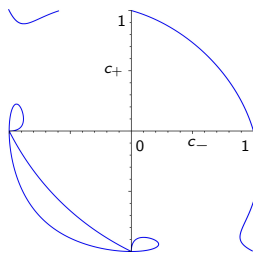
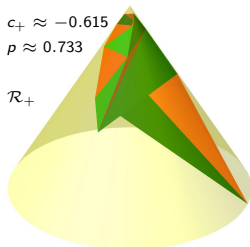
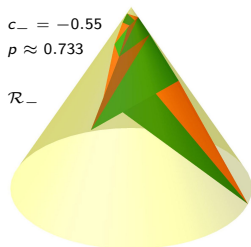
The planar curve h is of degree $n(n-1) - 6$.

2. **Special case:** $q = 0$

The planar curve h is of degree $(n-2)(n-3)$.

Remark 3: Multi-stable designs can only exist for $n > 3$.

Example 3: $n = 4$ and $\lambda_+ = \lambda_- = \frac{\pi}{6} \implies h$ is a sextic



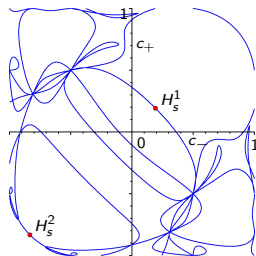
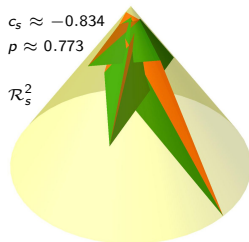
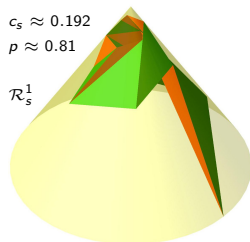
3a. Shaky realizations

Shaky realization \mathcal{R}_s are algebraically characterized by setting $c_s := c_- = c_+$ in the expression of h . The zeros of this univariate polynomial in c_s result in double solutions.

3a. Shaky realizations

Shaky realization \mathcal{R}_s are algebraically characterized by setting $c_s := c_- = c_+$ in the expression of h . The zeros of this univariate polynomial in c_s result in double solutions.

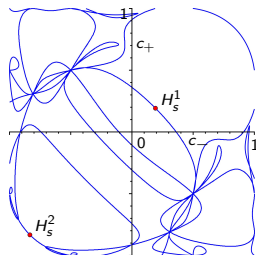
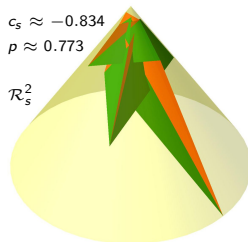
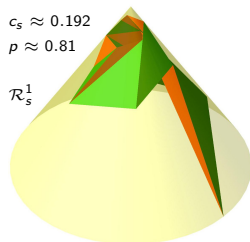
Example 4: $n = 6$ and $\lambda_+ = \lambda_- = \frac{\pi}{6} \implies h$ is of degree 24



3a. Shaky realizations

Shaky realization \mathcal{R}_s are algebraically characterized by setting $c_s := c_- = c_+$ in the expression of h . The zeros of this univariate polynomial in c_s result in double solutions.

Example 4: $n = 6$ and $\lambda_+ = \lambda_- = \frac{\pi}{6} \implies h$ is of degree 24



Remark 4: A geometric characterization of the shakiness remains an open problem. A necessary condition for the flat state ($\Leftrightarrow q = 0$) is that one of the two kinds of triangles has collinear vertices.

3b. Types of self-intersections

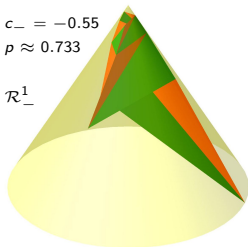
We call a self-intersection **local**, if triangles with a common vertex intersect each other; otherwise **global**.

3b. Types of self-intersections

We call a self-intersection **local**, if triangles with a common vertex intersect each other; otherwise **global**. Continuation of **Example 3**:

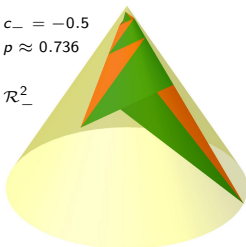
$$c_- = -0.55$$
$$p \approx 0.733$$

$$\mathcal{R}_-^1$$



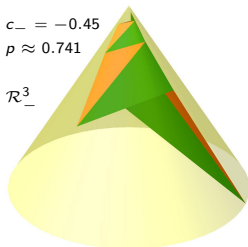
$$c_- = -0.5$$
$$p \approx 0.736$$

$$\mathcal{R}_-^2$$



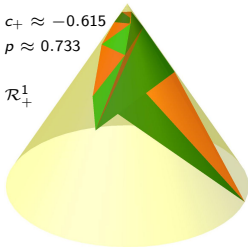
$$c_- = -0.45$$
$$p \approx 0.741$$

$$\mathcal{R}_-^3$$



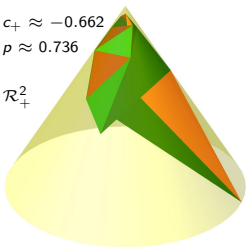
$$c_+ \approx -0.615$$
$$p \approx 0.733$$

$$\mathcal{R}_+^1$$



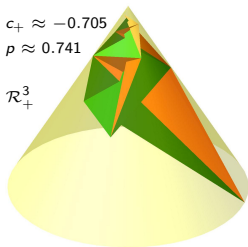
$$c_+ \approx -0.662$$
$$p \approx 0.736$$

$$\mathcal{R}_+^2$$



$$c_+ \approx -0.705$$
$$p \approx 0.741$$

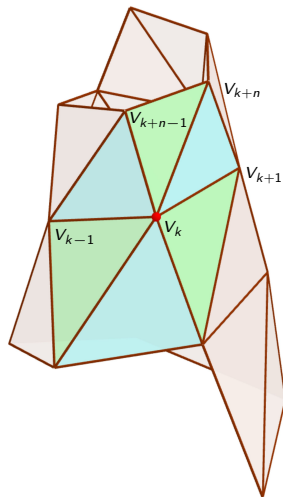
$$\mathcal{R}_+^3$$



3b. On local self-intersections

We consider the vertex star of V_k , which is split by the edges $V_{k-1}V_k$ and V_kV_{k+1} into two sets of three triangles; an upper set and a lower one. As the vertices are located on a spiral it is impossible that triangles of the upper set intersect triangles of the lower set and vice versa.

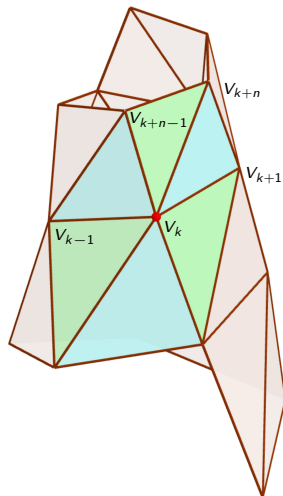
W.l.o.g. we can focus on the three triangles of the upper set of the vertex star.



3b. On local self-intersections

Let us assume that we start with a self-intersection free vertex star and deform it continuously such that the three triangles of the upper set intersect each other. The deformation has to pass a configuration, where two adjacent triangles of the upper set are coplanar (dihedral angle is zero).

This can happen along the edges $V_k V_{k+n-1}$ and $V_k V_{k+n}$. Hence there are two **boundaries of local self-intersection**.



3b. Theorem on local self-intersections

Theorem 1.

\mathcal{R}_- is a realization which is located on a right pyramid over a regular $(n-1)$ -gon or n -gon. If there exists a second realization \mathcal{R}_+ located on the same cone then it is on the boundary of local self-intersection.

3b. Theorem on local self-intersections

Theorem 1.

\mathcal{R}_- is a realization which is located on a right pyramid over a regular $(n-1)$ -gon or n -gon. If there exists a second realization \mathcal{R}_+ located on the same cone then it is on the boundary of local self-intersection.

Proof: This theorem was proven algebraically for $n = 4, \dots, 9$.

Clearly, one can try to prove this result for further values of $n > 9$, which is a cumbersome task due to the increasing degree of involved polynomials but the procedure is straight forward.

3b. Theorem on local self-intersections

Theorem 1.

\mathcal{R}_- is a realization which is located on a right pyramid over a regular $(n-1)$ -gon or n -gon. If there exists a second realization \mathcal{R}_+ located on the same cone then it is on the boundary of local self-intersection.

Proof: This theorem was proven algebraically for $n = 4, \dots, 9$.

Clearly, one can try to prove this result for further values of $n > 9$, which is a cumbersome task due to the increasing degree of involved polynomials but the procedure is straight forward.

Remark 5: We conjecture that this theorem holds for all $n > 3$ but an elegant proof (preferably a pure geometric one) remains open.

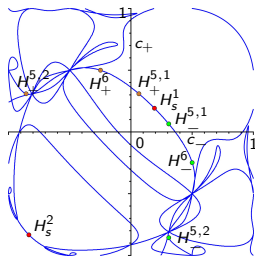
3b. Implications for global self-intersections

A snap of the framework on the cone corresponds to a path along the curve h between the point (a, b) and (b, a) . As a consequence such a snap has to pass a shaky realization \mathcal{R}_s .

Therefore the bounds of local self-intersection free realizations are given by \mathcal{R}_- located on right pyramid over a regular $(n - 1)$ -gon or n -gon and the shaky realization \mathcal{R}_s .

Hence, only these intervals can contain feasible candidates for a global self-intersection free snapping between two realizations.

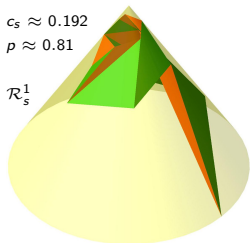
3b. Continuation of Example 4



$$c_s \approx 0.192$$

$$p \approx 0.81$$

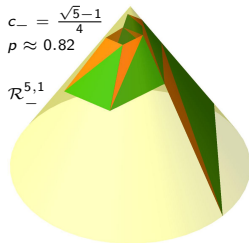
$$\mathcal{R}_s^1$$



$$c_- = \frac{\sqrt{5}-1}{4}$$

$$p \approx 0.82$$

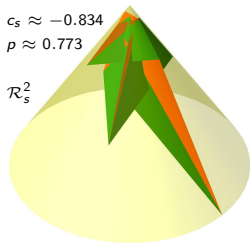
$$\mathcal{R}_-^{5,1}$$



$$c_s \approx -0.834$$

$$p \approx 0.773$$

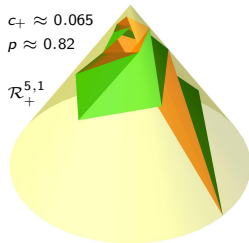
$$\mathcal{R}_s^2$$



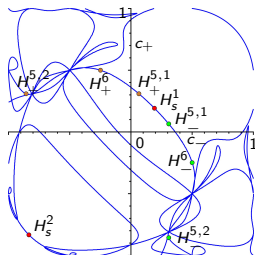
$$c_+ \approx 0.065$$

$$p \approx 0.82$$

$$\mathcal{R}_+^{5,1}$$

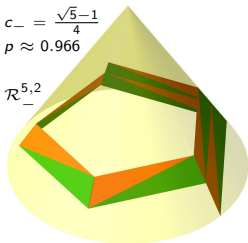


3b. Continuation of Example 4



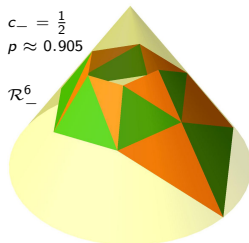
$$c_- = \frac{\sqrt{5}-1}{4}$$

$$p \approx 0.966$$

 $\mathcal{R}_-^{5,2}$


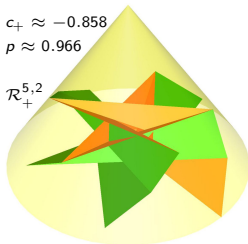
$$c_- = \frac{1}{2}$$

$$p \approx 0.905$$

 \mathcal{R}_-^6


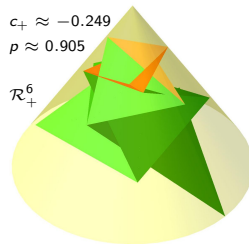
$$c_+ \approx -0.858$$

$$p \approx 0.966$$

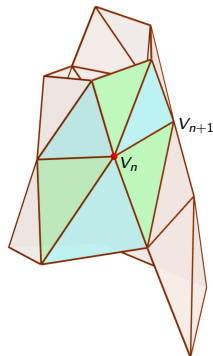
 $\mathcal{R}_+^{5,2}$


$$c_+ \approx -0.249$$

$$p \approx 0.905$$

 \mathcal{R}_+^6


4. Orthogonal cross sections



We compute the cross sectional area A of a realization \mathcal{R} , which is free of self-intersections.

Due to the kinematic construction we can restrict ourselves to cross sections, which intersect the line-segment $V_n V_{n+1}$. Then the intersection polygon consists of:

$$E_1 := V_n V_{n+1} \cap \varepsilon, \quad E_2 := V_1 V_{n+1} \cap \varepsilon, \quad E_3 := V_{n+1} V_2 \cap \varepsilon, \\ E_4 := V_2 V_{n+2} \cap \varepsilon, \dots \quad E_{2n-1} := V_{2n-1} V_n \cap \varepsilon, \quad E_{2n} := V_2 V_{2n} \cap \varepsilon$$

where ε denotes the cross sectional plane. Then we get A by:

$$A := \frac{1}{2} |\det(E_1, E_2) + \det(E_2, E_3) + \dots + \det(E_{2n-1}, E_{2n}) + \det(E_{2n}, E_1)|$$

4. Orthogonal cross sections

Theorem 2.

For any realization \mathcal{R} the expression A/h^2 is constant; i.e. it does not depend on the cut height h (distance of ε to the cone apex).

4. Orthogonal cross sections

Theorem 2.

For any realization \mathcal{R} the expression A/h^2 is constant; i.e. it does not depend on the cut height h (distance of ε to the cone apex).

Proof: This theorem was proven algebraically for $n = 3, \dots, 6$.

This result holds for any realization but only for self-intersection free ones a geometric interpretation for A as cross sectional area is available. In this case the volume is $hA/3$.

4. Orthogonal cross sections

Theorem 2.

For any realization \mathcal{R} the expression A/h^2 is constant; i.e. it does not depend on the cut height h (distance of ε to the cone apex).

Proof: This theorem was proven algebraically for $n = 3, \dots, 6$.

This result holds for any realization but only for self-intersection free ones a geometric interpretation for A as cross sectional area is available. In this case the volume is $hA/3$.

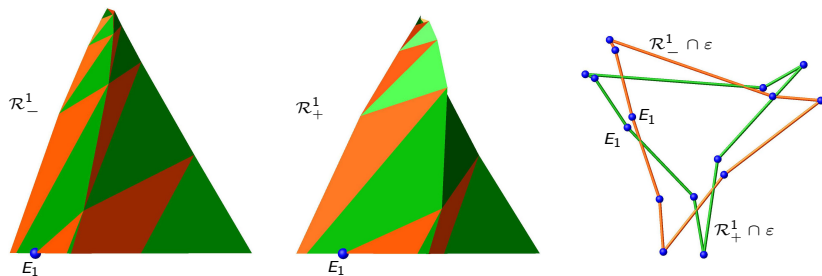
Remark 6: For a self-intersection free realization of a triangulated cylinder based on a helical arrangement it was proven by Wittenburg [12] (for $n = 3, \dots, 6$) that the area of the cross section (orthogonal to the cylinder axis) does not depend on the cut height.

4. Continuation of Example 3

We consider the two self-intersection free realizations \mathcal{R}_-^1 and \mathcal{R}_+^1 .

We cut both realizations at the height $h = -0.45$ and consider the conical structures above.

Both base polygons are visualized and their corresponding areas equals $A_- \approx 0.073$ and $A_+ \approx 0.051$, respectively.



5. Snappability computation

We study the snap between two realizations \mathcal{R}_+ and \mathcal{R}_- on the same cone, as these structures can change the cross-sectional area and volume while their conical shape is preserved.

5. Snappability computation

We study the snap between two realizations \mathcal{R}_+ and \mathcal{R}_- on the same cone, as these structures can change the cross-sectional area and volume while their conical shape is preserved.

Assumption: As in the study [2] by Guest and Pellegrino on the analogue construction for the cylindrical case, we assume that the folding process is *uniform*; i.e. the vertices remain on a spiral curve during the deformation.

5. Snappability computation

We study the snap between two realizations \mathcal{R}_+ and \mathcal{R}_- on the same cone, as these structures can change the cross-sectional area and volume while their conical shape is preserved.

Assumption: As in the study [2] by Guest and Pellegrino on the analogue construction for the cylindrical case, we assume that the folding process is *uniform*; i.e. the vertices remain on a spiral curve during the deformation.

The snappability index [8], which measures the snapping capability of the structure, is based on the following property:

The snap between two realizations \mathcal{R}_+ and \mathcal{R}_- has to pass a shaky configuration \mathcal{R}_s at the maximum state of deformation with respect to the total elastic strain energy. The snappability ς equals the total elastic strain energy density of \mathcal{R}_s .

5. Snappability computation

By using results for geometric series we can compute the snappability of these infinite structures in two ways:

1. **Rough computation:** \mathcal{R}_s is assumed to be on the same cone.
2. **Improved computation:** No assumption on \mathcal{R}_s

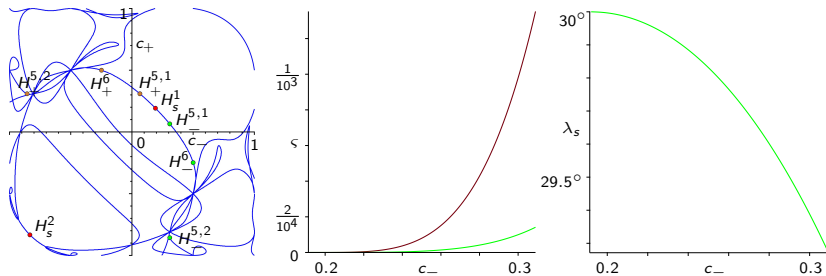
5. Snappability computation

By using results for geometric series we can compute the snappability of these infinite structures in two ways:

1. **Rough computation:** \mathcal{R}_s is assumed to be on the same cone.
2. **Improved computation:** No assumption on \mathcal{R}_s

Continuation of **Example 4:**

We consider the set of global self-intersection free snapping realizations, i.e. curve segment of h bounded by $H_-^{5,1}$ and H_s^1 .



6. Open problems

- Geometric proofs of Theorems 1 and 2 for all n .
- Geometric characterization of shaky configurations.
- Existence of three self-intersection free realizations on different cones?
- Conjecture: There are at most two realizations on the same cone.
- Generalization to polyhedral cone surfaces with quadrilateral faces in analogy to cylinders formed from Kokotsakis' flexible tessellations [10].

Acknowledgment

The author is supported by grant P 30855-N32 of the Austrian Science Fund FWF as well as by FWF project F77 (SFB "Advanced Computational Design", subproject SP7).

6. References

- [1] Cai, J., Deng, X., Zhang, Y., Feng, J., Zhou, Y.: Folding behavior of a foldable prismatic mast with Kresling pattern. *Journal of Mechanisms and Robotics* **8** 031004 (2016)
- [2] Guest, S.D., Pellegrino, S.: The folding of triangulated cylinders, Part I/II. *Journal of Applied Mechanics* **61**(4) 773–777/778–783 (1994)
- [3] Hunt, G.W., Ario, I.: Twist buckling and the foldable cylinder: an exercise in origami. *Int. Journal of Non-Linear Mechanics* **40** 833–843 (2004)
- [4] Ishida, S., Nojima, T., Hagiwara, I.: Mathematical approach to model foldable conical structures using conformal mapping. *Journal of Mechanical Design* **136** 091007 (2014)
- [5] Kresling, B.: Natural twist buckling in shells: from the Hawkmoth's bellows to the deployable Kresling-pattern and cylindrical Miura-ori. *Proc. of the 6th International Conference on Computation of Shell and Spatial Structures* (J.F. Abel, J.R. Cooke eds.), Ithaca, NY (2008)
- [6] Liu, K., Paulino, G.H.: Nonlinear mechanics of non-rigid origami: an efficient computational approach. *Proceedings of the Royal Society A* **473**(2206) 2017.0348 (2017)

- [7] Liu, X., Yao, S., Georgakopoulos, S.V.: Reconfigurable origami equiangular conical spiral antenna. In Proc. of 2015 IEEE International Symposium on Antennas and Propagation & USNC/URSI National Radio Science Meeting, pages 2263–2264 (2015)
- [8] Nawratil, G.: Snappability and singularity-distance of pin-jointed body-bar frameworks. Mechanism and Machine Theory **167** 104510 (2022)
- [9] Nojima, T.: Origami Modeling of Functional Structures based on Organic Patterns. Presentation Manuscript at VIPSI Tokyo (2007)
- [10] Stachel, H.: A Flexible Planar Tessellation with a Flexion Tiling a Cylinder of Revolution. Journal of Geometry Graphics **16**(2) 153–170 (2012)
- [11] Whirlwind: <https://www.instructables.com/The-Whirlwind-An-iPhone-horn-speaker-and-stand-t/>
- [12] Wittenburg, J.: Foldable and Self-Intersecting Polyhedral Cylinders Based on Triangles. Journal for Geometry and Graphics **23**(2) 245–258 (2019)
- [13] Wunderlich, W.: Snapping and Shaky Antiprisms. Mathematics Magazine **52**(4) 235–236 (1979)